

## **Peptides as Biosorbents - Promising tools for resource recovery**

Braun, R.; Bachmann, S.; Schönberger, N.; Matys, S.; Lederer, F.; Pollmann, K.;

Originally published:

June 2018

**Research in Microbiology 169(2018)10, 649-658**

DOI: <https://doi.org/10.1016/j.resmic.2018.06.001>

Perma-Link to Publication Repository of HZDR:

<https://www.hzdr.de/publications/Publ-27183>

Release of the secondary publication  
on the basis of the German Copyright Law § 38 Section 4.



1 **Abstract.**

2 Despite many innovations, meeting both economic and ecological requirements remains  
3 challenging for conventional resource recovery technology. The development of highly  
4 selective peptides puts a new competitor on the market. We present an approach to identify  
5 peptides for resource recovery using Phage Surface Display. Here, we describe the  
6 development of peptides for binding of rare earth element terbium-containing solids and for  
7 removal and enrichment of the heavy metal ions of cobalt and nickel out of waste waters and  
8 leaching solutions.

9

10 **Keywords:** phage display; biosorption; peptide; biohydrometallurgy

11

## 1 **Introduction.**

2 Usage of biology in mining was first commercially applied in the 1950s, when the  
3 exploitation of bacteria for copper extraction was patented. Since then dump bioleaching is  
4 the fundamental part for the extraction of valuables from marginal-grade ore. Heap  
5 bioleaching and stirred-tank bioextraction were utilized commercially beginning in the 1980s  
6 [1]. The increasing importance of biomining regarding the growing usage of bacteria and  
7 described reaction principles were comprehensively reviewed by Bosecker (1997) [2] and  
8 Johnson [3,4]. Even extraction of valuables from non-mineral resources as metallic wastes are  
9 nowadays being discussed. For most processes and bacteria used, even the molecular  
10 pathways are very well described and the intra-bacterial mechanism are known in detail [5].  
11 However, up to now, biomining only covered the usage of bacteria. Bacteria are complex  
12 living constructs with constant need for substrates, changing demands and reactions  
13 depending on the conditions used for metal recovery. Interaction of metals and bacteria is  
14 mostly accomplished by different proteins and enzymes, such as cytochromes [6], with redox  
15 pathways typically used for bioleaching only contributing a small part to the complete  
16 metabolism. Unlike in bioleaching, where binding of target elements and redox  
17 transformations are equally important, in biosorption binding of target substances is of main  
18 importance. As a result, systems using chemicals with functionalities borrowed from nature  
19 are already being applied for bioflotation or e.g. flocculation. Therefore, the potential use of a  
20 proteinic biological system, which only provides metal binding capacity would benefit from  
21 leaving behind other biological fluctuations. It also becomes more attractive, as peptides and  
22 proteins usually show high sensitivity and selectivity towards their target molecules. For most  
23 biohydrometallurgical purposes acidification is also necessary, which is wasteful and not  
24 required anymore when only the metal-binding proteins are being used. Other biological  
25 molecular systems using complexing molecules, which are available for biosorption are e.g.  
26 siderophores [7].

27 In this study, we describe how to select und utilize only the protein domains, which are  
28 obligatory for metal-interaction using Phage Surface Display (PSD). In the last decades PSD  
29 has mainly been used in medical context such as the discovery of diagnostic and therapeutic  
30 peptides e.g. for the recognition of cancer. However growing interest is nowadays drawn to  
31 the identification of inorganic binding peptides [8], e.g. hydroxyapatite for medical devices.  
32 Phage Surface Display uses the unique characteristic of phage, the combination of genotype  
33 (DNA encoding the phage structure) and phenotype (the proteinic structure of the phage)  
34 without the influences of living nature. Every living cell possesses a metabolism. It is

1 subjected to a constantly changing environment resulting in a constantly changing structure of  
2 the cells. Phage however, can be considered as a molecular building block as they show no  
3 metabolism and variability of structure. For PSD, a DNA sequence coding for a short peptide  
4 motif, is added to DNA sequence of the coat proteins of the phage, resulting in phage  
5 displaying these short peptide motifs. Libraries of phage can be created that include billions  
6 of different sequence motifs, which can be used for the identification of target-specific  
7 peptides.

8 Recently, usability of PSD for solid- and inorganic material binding was shown and is well  
9 summarized in the reviews of Seker & Demir (2011) and Care et al. (2015) [9,10]. However,  
10 application areas were mainly described in medicine and nanotechnology, e.g. for biosensors  
11 and biomaterials. With this work, we expand the usability of PSD and the boundaries of  
12 biomining by identification and characterization of peptides that are binding to metal ions  
13 from waste waters and leachates as well as binding to solids, e.g. from solid scrap for the  
14 recovery of rare earth element (REE)-containing compounds as shown in Fig. 1.  
15 Perspectively, these peptides can be addressed to genetic engineering for adaption and  
16 modification, e.g. for immobilization and reusability or to simplify heterologous production.

17

## 1 **Materials and methods.**

2 *Phage libraries and bacterial strains.* Experiments for the identification of terbium-binding  
3 peptides were performed using the LX-4 library, a random PVIII phage library, kindly  
4 provided by Dr. Jamie Scott (Simon Fraser University, Burnaby, BC) [11]. Selection of phage  
5 and peptide sequences able to bind to nickel or cobalt was performed with the Ph.D.<sup>TM</sup>-C7C  
6 phage library (NEB, US), displaying randomized peptides on the PIII coat protein. All  
7 displayed peptides possess the amino acid sequence ACXCGGG, with X being a motif of  
8 seven randomized amino acids. The bacterial strain used for phage amplification was *E. coli*  
9 ER2738 (*F'* *proA*<sup>+</sup>*B*<sup>+</sup> *lacI*<sup>q</sup>  $\Delta$ (*lacZ*)*M15* *zzf::Tn10(Tet<sup>R</sup>)/fhuA2* *glnV*  $\Delta$ (*lac-proAB*) *thi-1*  
10  $\Delta$ (*hsdS-mcrB*)5).

11 *Phage Surface Display for solid-binding peptides.* Terbium doped cerium-magnesium  
12 aluminate (CAT) (Leuchtstoffe Breitung GmbH, Germany), an indispensable part of  
13 fluorescent powder of compact light bulbs, was used for the selection of specific binding  
14 peptides out of recombinant phage library. Experiments were performed as described  
15 elsewhere [12,13]. The main steps are summarized below, for detailed descriptions please  
16 refer to Lederer et al. (2017). Samples of CAT were washed and subsequently blocked with  
17 Tween 20 and BSA. After extensive washing  $\sim 2 \times 10^{11}$  phage particles displaying  
18  $1.5 \times 10^9$  different randomized peptides were incubated with the pretreated mineral. Removal  
19 of weakly bound phage was achieved by subsequent repeated washing. Elution of strong  
20 binding phage was carried out by lowering the pH or alternatively achieved by incubating the  
21 material directly with freshly prepared *E. coli* cells. Amplification of phage was achieved by  
22 infection of freshly prepared *Escherichia coli* K91 [14]. Infected cells were cultivated and  
23 induced with IPTG. Isolation of produced phage particles was performed via PEG  
24 precipitation as described elsewhere [14]. Enrichment of specific binding phage usually  
25 requires several rounds of biopanning with enhanced stringency to select strongly binding  
26 phage. Therefore, three rounds of biopanning were performed with increasing concentration  
27 of Tween 20 in binding and washing buffer. After completion of three rounds of biopanning,  
28 phage containing supernatant of colonies of infected *E. coli* cells was used as template for  
29 PCR amplification.

30 *Phage Surface Display for ion-binding peptides.* The biopanning selection process of phage  
31 for ion specific binding has been accomplished using planar sol gel materials (GMBU e.V.,  
32 Germany) with ion exchange properties. Experiments and preparations were carried out as  
33 described by Schönberger et al. 2017 [15]. Sol gel materials were prepared with cationic

1 binding capacity using tetraethylorthosilicate (TEOS) and different polymers (15 % w/w  
2 Dispex N40, polyacrylic acid or polystyrene sulfonate). For biopanning the sol gel materials  
3 were loaded with divalent nickel or cobalt-salt containing buffers. Preparation, binding  
4 procedure, washing steps and elution were performed as described by Schönberger et al.  
5 Selection pressure in the different biopanning rounds was accomplished by lowering the pH.  
6 Elution was alternatively achieved by incubating the material directly with freshly prepared *E.*  
7 *coli* ER2738 cells. Amplification of phage was performed as described elsewhere [14]. After  
8 determination of phage concentration, the supernatant of the phage containing, infected  
9 colonies of *E. coli* cells was used as template for PCR amplification.

10 *Sequencing.* Sanger sequencing was carried out by GATC Biotech AG (Germany). For the  
11 LX-4 phage library oligonucleotide primers were: (forward) 5'-  
12 GCTCTAAATCGGGGGAGCT-3'; (reverse) 5'-  
13 CATAAGCTAGCTTAAAAAAAAGCCCGC-3'. For Ph.D.<sup>TM</sup>-C7C phage libraries  
14 oligonucleotide primers were: (forward) 5'-GCAACTATCGGTATCAAGCT-3'; (reverse) 5'-  
15 CCCTCATAGTTAGCGTAACG-3'. Amplified PCR products were used for sequencing and  
16 identification of recombinant peptide sequences. The primer sequences used for Sanger  
17 sequencing were 5'-CCCTCATAGTTAGCGTAACG-3' (C7C) and 5'-  
18 AGTAGCAGAAGCCT- GAAGA-3' (LX-4).

19 *Binding Assay for solid-binding peptides.* Pre-identified phage, derived from single clone  
20 amplification out of colonies of infected cells, were characterized concerning their ability to  
21 bind to individual components of fluorescent lamp powder and to quantify the selective  
22 binding behavior. Components tested were CeMgAl<sub>11</sub>O<sub>19</sub>:Tb<sup>3+</sup> (CAT), Y<sub>2</sub>O<sub>3</sub>:Eu<sup>3+</sup> (YOX),  
23 BaMgAl<sub>10</sub>O<sub>17</sub>:Eu<sup>2+</sup> (BAM), LaPO<sub>4</sub>:Ce,Tb (LAP) and halophosphate (HP). Mineral  
24 preparation, phage production and binding studies were performed as described elsewhere  
25 [12]. Mineral dispersions were incubated together with the phage and subsequently repeatedly  
26 washed, resulting in the removal of weakly bound phage. Phage concentrations in input and  
27 eluate were determined and compared to the binding behavior of wild-type fd-tet phage  
28 (obtained by Dr. Jamie Scott). Calculated values describe the ratio of bound phage in eluate  
29 compared to phage input concentration normalized against the wild-type phage values. The  
30 binding assay for cobalt and nickel-binding phage was conducted as described here, however  
31 nitrilotriacetic acid (NTA) sepharose with either immobilized nickel or cobalt was used as  
32 binding material. Same buffers as in the preceding biopanning experiments were used.

1 *Competitive Binding.* Competitive binding characterization was done using defined phage  
2 libraries of amplified phage. Libraries were created by using equimolar concentrations of  
3 phage ( $1 \times 10^{10}$  Pfu mL<sup>-1</sup>), which have previously been identified in the biopanning process.  
4 The method was performed as described earlier [12,16].

5 *Immunofluorescence.* Fluorescence microscopy (Olympus; Japan). was used to compare the  
6 intensity of emitted fluorescence of minerals and phage, which were treated with fluorophore-  
7 labeled antibodies. Phage were firstly marked with a primary, phage-binding antibody, which  
8 was subsequently treated with a secondary fluorophore-labeled antibody, specifically binding  
9 the primary antibody. Preparation of CAT mineral, phage binding, washing and sample  
10 preparation for microscopy were performed as described by Lederer et al. (2017) [12].

11

## 1 **Results.**

2 *Solid-binding peptides.* Random peptide sequences with high affinity to CAT minerals were  
3 identified from the PVIII phage library LX-4. After three rounds of biopanning corresponding  
4 DNA sequences of the displayed peptides on phage of 80 infected colonies were amplified via  
5 PCR and sequenced. 11 different sequences were determined which generally showed a high  
6 content of amino acids with charged side-chains, especially lysine. KKQKCRTDACVTQM  
7 was the most-occurring sequence and was found 7 times, other sequences were found only  
8 with lower frequency. Table 1 shows a list of all identified sequences and the general  
9 composition of their amino acid sequences. All identified peptides possess a high proportion  
10 of charged, hydrophilic amino acids while hydrophobic and acidic amino acids are absent or  
11 occur in low frequency. For further characterization of the binding affinity of the peptides to  
12 CAT minerals, a competitive binding assay was carried out. 30 colonies of infected bacteria  
13 were characterized in regards of the displayed peptide sequence. Results can be found in  
14 Table 1. Interestingly the monitored sequence frequencies strongly differ from the relative  
15 occurrence of peptides after panning with the original library. Peptides, which were originally  
16 found in smaller proportions now contribute to nearly half of all identified sequences. Most of  
17 the identified peptide sequences resemble in their theoretical isoelectric point being above 8.8  
18 resulting in a positive net electrical charge at pH 7.5, which was chosen for biopanning. The  
19 most frequent sequences KKQKCRTDACVTQM (SB1), NEKKCKGARCTTVT (SB2),  
20 ATPKCKKKSCMTTQ (SB3) and ETKKCTTGPCVVVT (SB4) were chosen for further  
21 binding assays.

22 Binding of amplified phage as ratio of phage input titer and phage elution titer was  
23 determined with CAT minerals for at least three times. Results are shown in Fig. 2. All tested  
24 phage had a higher binding efficiency against the tested materials as wild-type phage,  
25 indicating that preceded biopanning had successfully selected peptide sequences with high  
26 affinity to CAT. Measured binding efficiencies of sequences NEKKCKGARCTTVT (SB2  
27  $84.3 \pm 19.4$ ), ATPKCKKKSCMTTQ (SB3  $94.5 \pm 29.9$ ) and KKQKCRTDACVTQM (SB1  
28  $128.6 \pm 23.5$ ) were in a similar range, while binding efficiency of ETKKCTTGPCVVVT  
29 (SB4  $13.4 \pm 4.7$ ) was only slightly increased in comparison to the wild-type binding  
30 properties. Although being dominant in the competitive occurrence measurements, the  
31 binding efficiency was more similar to the wild-type phage than to the other identified  
32 sequences.

1 Immunofluorescence labeling was performed to visualize the binding and to describe the  
2 distribution of bound phage, as shown in Fig. 3. Phage SB1 displaying the peptide  
3 KKQKCRTDACVTQM and wild-type phage were incubated with CAT and marked with the  
4 antibodies. CAT mineral is showing autofluorescence at 360 – 410 nm (filter U-MNU),  
5 however with filter U-N39010 (540 – 580 nm) fluorescence of the secondary antibody can be  
6 visualized. In Fig. 3 phase contrast and fluorescence microscopy pictures using different  
7 filters are shown. CAT minerals used had a size of 5 – 15  $\mu\text{m}$ . Visualization of phage was  
8 possible with filter U-N39010 showing high fluorescence in picture B3 which is somewhat  
9 reduced after elution (compare B6). Only weak fluorescence was detected for CAT mineral  
10 treated with wild-type phage, which further decreased after the elution. Similar effects were  
11 seen for Phage SB2, SB3 and SB4 (results not shown).

12 Besides the binding ability to CAT, peptides for future industrial purposes may need to  
13 discriminate between different materials. Therefore binding studies with  $\text{CeMgAl}_{11}\text{O}_{19}:\text{Tb}^{3+}$   
14 (CAT),  $\text{Y}_2\text{O}_3:\text{Eu}^{3+}$  (YOX),  $\text{BaMgAl}_{10}\text{O}_{17}:\text{Eu}^{2+}$  (BAM),  $\text{LaPO}_4:\text{Ce}^{3+},\text{Tb}^{3+}$  (LAP) and  
15 halophosphate (HP) were conducted, materials typically found in fluorescent lamp powder.  
16 Results are shown in Fig. 4. Binding efficiency was calculated using phage titer before and  
17 after binding assays in comparison to the wild-type phage. Peptide sequences used for  
18 comparison were KKQKCRTDACVTQM, NEKKCKGARCTTVT, ATPKCKKKSCMTTQ  
19 and ETKKCTTGPKVVT, which were predominantly identified either in original  
20 biopanning experiments or in subsequent competitive binding experiments using mini  
21 libraries.

22 Binding behavior towards different materials differs between the tested phage. All tested  
23 sequences show a higher affinity towards CAT compared to wild-type phage (compare  
24 Table 1). While the binding affinity towards LAP and BAM of SB1 is equally high as for  
25 CAT (LAP  $126 \pm 6$ , BAM  $148 \pm 7$ , CAT  $128 \pm 23$ ), both SB2 and SB3 show a specific  
26 binding affinity towards CAT, which is ~ 3 times higher as the normalized binding efficiency  
27 towards LAP and BAM. However, it has to be highlighted, that binding efficiencies for both  
28 materials and peptide sequences are strongly increased compared to the wild-type binding  
29 behavior (SB2: LAP  $28 \pm 3$ , BAM  $29 \pm 6$ ; SB3: LAP  $31 \pm 0$ , BAM  $39 \pm 2$ ). Binding affinities  
30 for SB4, which showed dominant occurrence in competitive binding assays, follow another  
31 trend. While the peptide sequence does only show a slight increase in binding efficiency  
32 towards CAT ( $13 \pm 5$ ) and LAP ( $4 \pm 2$ ), affinity for BAM is drastically increased compared to  
33 the wild-type phage ( $58 \pm 37$ ). All tested phage possessed affinities to YOX and  
34 halophosphate, which are comparable with the wild-type phage behavior. Consequently, only

1 phage displaying the sequences SB2 and SB3 can be considered as selective for CAT in the  
2 range of tested materials. While SB1 shows equally good binding affinities for CAT, LAP and  
3 BAM, SB4 even shows a higher affinity to BAM compared to CAT.

4 *Ion-binding peptides.* Metal ions such as cobalt(II) and nickel(II) ions were chosen as another  
5 target for phage selection. Peptides specifically binding these ions are attractive bioligands for  
6 the construction of biosorptive materials. Biopanning was carried out on planar sol-gel  
7 surfaces. Sol-gels with cation exchange properties were fabricated using Dispex N40,  
8 polyacrylic acid or polystyrene sulfonate, as described elsewhere [17]. Selection pressure for  
9 peptide identification was achieved using lowered pH values over the biopanning rounds. In  
10 Table 2 all identified peptide sequences as well as their frequencies are shown. The theoretical  
11 pI of the peptide, calculated with ExPASy ProtParam [18] and the general amino acid  
12 composition are shown because the net charge of the peptide and properties of amino acid  
13 side chains have a high impact on the binding behavior. In the biopanning experiments that  
14 were performed in order to identify cobalt (II)-binding peptides, 63 colonies were examined  
15 for their peptide sequence. 28 unique sequences were identified, whereof 22 sequences  
16 occurred only once. The peptides sequence MSTGLSS (SMC01) occurred 28 times,  
17 constituting nearly half of all analyzed sequences. Further the sequence VPILEGT (SMC02)  
18 was identified 5 times, and the peptides DRTISNK (SMC03), QNPGNTL (SMC04),  
19 SGTGASY (SMC05) and SSSVVTH (SMC06) were found with each two times. Especially  
20 the more frequent sequences except DRTISNK (SMC03) possess a low theoretical pI around  
21 4 – 5.5. All sequences also have a relatively high content of hydroxylic and polar amino acids,  
22 while charged amino acids are only found in smaller numbers and aromatic amino acids are  
23 nearly absent. Especially in case of sequences that are found only once, the theoretical pI  
24 shows a clear difference to more abundant sequences, having values of 8 or higher. In  
25 comparison, sequences that were identified to bind to nickel (II) ions generally show a more  
26 equal distribution. 29 colonies were sequenced and 24 unique peptide sequences were  
27 identified. Only SGTGASY (SMN01) occurred 3 times, whereas MSTGLSS (SMN02),  
28 NTGSPYE (SMN03) and TASQNFY (SMN04) each were identified two times. The general  
29 properties of the identified nickel-binding peptides are similar to the cobalt-binding peptides.  
30 In particular, the peptides have high contents of hydroxylic and polar amino acids whereas  
31 charged amino acids occur only in minor amounts and aromatic amino acids are nearly  
32 absent. Especially peptide motifs with a higher frequency show a relatively low theoretical pI  
33 of about 5, while the other sequences possess pI values typically > 8 but within a range of 4 –  
34 11.

1 The binding properties of the identified peptide motifs were determined by performing  
2 binding assays comparing phage input titer and phage titer in elution fractions after extensive  
3 washing. Measured values were normalized against the binding behavior of wild-type phage.  
4 Results are graphically shown in Fig. 5 A and are listed in detail in Table 2. Binding  
5 experiments were performed only for the most promising sequence motifs. As shown in Fig.  
6 5A the normalized binding efficiencies of nickel-binding motifs were 18 times higher  
7 compared to the wild-type. Interestingly two motifs with the strongest binding efficiency  
8 towards nickel (SMN06, SMN12) both occurred in the biopanning with a frequency of 01/29  
9 and possess a pI above 8. The three peptide motifs SMN4, SMN01, SMN02, occupying the  
10 second place in terms of binding affinity, were found with a frequency of 02/29 in the  
11 preceding biopanning. All three peptides possess a pI of about 5. In addition, many sequence  
12 motifs were identified that show a binding behavior comparable to the wild-type even after  
13 three rounds of biopanning with increased selection pressure. Distribution of cobalt-binding  
14 peptide motifs was more uniform as shown in Fig. 5 B. Identified sequences showed a  
15 binding efficiency with 0.8 – 3.1 times higher than the wild-type. Sequences occurring with  
16 higher frequency generally showed a stronger binding affinity (compare SMC01, SMC04,  
17 SMC06). However, the strongest binding peptide motif SMC28 was found only once in the  
18 preceding biopanning. Stronger binding sequences tended to possess a theoretical pI of about  
19 5.

20 As peptides for resource recovery need to be sensitive and selective, promising candidate  
21 motifs were used for further binding assays. Peptides, which were originally identified as  
22 nickel-binding sequences, were characterized for their binding efficiency towards cobalt and  
23 vice versa. In Fig. 6 selected sequences are compared regarding their binding affinities.  
24 Besides the normalized binding efficiency, the ratios of efficiencies for nickel and for cobalt  
25 are displayed. Some sequences (e.g. SMC15) bound nickel and cobalt in similar amounts,  
26 even if they were identified only in the biopanning for one of the heavy metal ions.  
27 Interestingly, the affinity of e.g. SMC17, which was selected as cobalt-binding peptide, to  
28 nickel is even higher. In contrast, SMC12 that was selected as cobalt-binding peptide, shows a  
29 high affinity for cobalt and a lower affinity to nickel.

30

## 1 **Discussion.**

2 *Solid-binding peptides.* Peptide sequences with a high affinity towards CAT mineral were  
3 identified from the PVIII phage library LX-4. Frequency of the identified phage differed from  
4 01/80 to 07/80. Sequences chosen for further experiments had a frequency of at least 03/80  
5 with the exception of SB4. This motif showed an initial frequency of 01/80 in the original  
6 biopanning but its occurrence in competitive binding assays drastically increased to 14/30,  
7 being the most abundant sequence in this assay. pI of all identified motifs was found to be  
8 above 8.8 with the exception of VDKKCKSDDCGAWH (theoretical pI 6.7). All sequences  
9 showed a high content of hydrophilic and basic amino acids. Acidic and hydrophobic amino  
10 acids were only found in small numbers with aromatic amino acids being nearly absent,  
11 although acidic amino acids were highly over-represented in peptides discovered by Ploss et  
12 al. to bind to metallic borides [16]. A high content of polar amino acids is consistent for all  
13 identified motifs. Especially the charged side-chains indicate a surface charge of the CAT  
14 minerals used for biopanning. As described by Curtis et al. [13], charged and polar amino  
15 acids interact with REE material. The basic amino acid mainly found was lysine (K) with no  
16 identified sequence containing less than three lysine. As the pK of the  $\epsilon$ -amino group is at  
17 10.28, it shows a positive charge at pH 7.5 chosen for biopanning. However, pK  $\sim$  6.0 of the  
18 imidazole side chain of histidine results in a negative charge of the amino acid at pH 7.5. Low  
19 occurrence of acidic amino acids may be due to the chosen experimental setup with the pH  
20 strongly affect the properties of these side-chains. One underlying mechanism may be  
21 electrostatic interaction, as shown by Hatanaka for peptide interaction with charged REE [19].  
22 Chen showed, that the binding mechanism of several metal oxides was of electrostatic nature  
23 [20]. Also, Rosi and Chen described electrostatic interaction to be the main interaction  
24 principle between inorganic materials and peptides besides complexation by protein folding  
25 [21].

26 Affinity towards CAT mineral was determined for peptide sequences SB1, SB2, SB3 and SB4  
27 which occurred predominantly in either original biopanning experiments or in the following  
28 competitive binding assays. Sequences SB1, SB2 and SB3 showed a strongly increased  
29 binding efficiency compared to wild-type, at least 80fold higher, whereas SB4 showed a  
30 slightly higher affinity ( $\sim$ 10 fold). Interestingly, SB4 was predominantly found in the  
31 competitive binding assay, an additional round of biopanning. These shifts in the peptide  
32 composition and motif frequency within phage libraries can be the result of the phage  
33 amplification in *E. coli*, which is necessary for further panning rounds. However, every  
34 amplification step introduces a library bias, as previously described [22,23]. Amplification

1 principles in bacteria differ from the biopanning selection pressure. Codon usage, amino acid  
2 preferences for bacterial infection, transport processes and protein folding strongly influence  
3 the composition of the phage library. Therefore amplification processes, although necessary,  
4 need to be minimized. High occurrence and relatively low binding properties occur most  
5 likely because of the previously discussed amplification bias, impressively illustrating the  
6 influence of only one additional amplification step. Bakhshinejad et al. demonstrated, that this  
7 loss-of-function may be the result of amplification advantages of fast-propagating phage over  
8 slow-propagating phage. Another explanation of the binding behavior and high abundance of  
9 SB4 may be, that adsorption to plastic surfaces [24] and albumin [25] cannot be prevented  
10 and may result in enrichment of phage with off-target binding affinities.

11 Immunofluorescence did show the superior binding behavior of chosen phage SB1. High  
12 fluorescence of antibody-marked phage could be measured on CAT material treated with  
13 SB1, with little to no fluorescence detection of CAT treated with wild-type phage (compare  
14 Fig. 3 A3, B3). Even after elution, detection of high fluorescence was still possible, because  
15 strongly bound phage could not be removed with chosen elution conditions. These findings  
16 indicate, that SB1 might be a “super-binder” showing very high and resistant affinity to the  
17 target material. Similar results were described by Lederer et al. [12].

18 For further characterization of the materials selectivity of identified peptide sequences,  
19 binding assays were performed with  $\text{CeMgAl}_{11}\text{O}_{19}:\text{Tb}^{3+}$  (CAT),  $\text{Y}_2\text{O}_3:\text{Eu}^{3+}$  (YOX),  
20  $\text{BaMgAl}_{10}\text{O}_{17}:\text{Eu}^{2+}$  (BAM),  $\text{LaPO}_4:\text{Ce}^{3+},\text{Tb}^{3+}$  (LAP) and halophosphate (HP), materials  
21 typically found in fluorescent lamp powder. For SB1, binding affinities towards LAP and  
22 BAM were equally high compared to CAT, while SB2 and SB3 did show high selectivity  
23 towards CAT with binding efficiencies being around three times higher in comparison to the  
24 other tested materials. SB4 however did show highest affinity for BAM, indicating that the  
25 mineral samples, which were chosen for biopanning may have been contaminated with BAM.  
26 However, this may not necessarily be true, as characteristics of CAT and BAM show  
27 similarities. Inorganic materials as CAT and BAM possess a complex structure, which may  
28 interfere with phage binding resulting in difficult biopanning experiments with e.g. the false  
29 positive identification of off-target binding phage [26]. In conclusion, peptide motifs  
30 specifically binding CAT as well as motifs binding a broader range of REE-containing  
31 materials were identified, paving the way to biotechnological solutions for REE recovery.

32 *Ion-binding peptides.* Besides the characterization of solid REE-binding peptides, we present  
33 the identification of peptide sequences for binding of the heavy metal ions of nickel and

1 cobalt. Following the biopanning on planar sol-gel material with ion exchange capacity, 28  
2 unique potentially cobalt-binding sequences were discovered. With a frequency of 28/63  
3 MSTGLSS was the most abundant peptide sequence, followed by VPILEGT with 5/63. Four  
4 additional motifs were found with a frequency of 2/63. All discovered sequences consist of no  
5 to little numbers of aromatic amino acids. Different contents of hydrophobic, charged, polar  
6 and hydroxylic amino acids are found in the discovered motifs. Especially the high abundant  
7 sequences share a theoretical pI ~ 5. The lack of aromatic amino acids is in contradiction to  
8 the findings of Ueda et al., who described tryptophan (W), phenylalanine (F) and tyrosine (Y)  
9 to have high metal ion affinity because of their aromatic amino acid side chains. Additionally  
10 histidine (H) and cysteine (C) did show the highest affinity to metal ions, while both are  
11 rarely found in our results [27,28]. However, Ph.D.<sup>TM</sup>-C7C phage libraries naturally include  
12 two cysteines, which form a disulfide bridge, flanking the peptide motifs and possibly  
13 interacting with metal ions. Especially for cysteine these findings arise from the fact, that  
14 unpaired cysteines do have negative effects on phage infection, hence unpaired cysteine-  
15 containing peptides cannot be found in the biopanning results as they add negative selection  
16 pressure to the containing peptides and may even not be present in the original library [29],  
17 even though it was described to interact with Cu(II) [30]. Cobalt(II), nickel(II) and copper(II)  
18 are also generally used for immobilization of histidine-containing peptides and proteins  
19 [31,32]. This explains why histidine is found in the identified peptide motifs, however  
20 quantity was lower than expected. When compared to the retention properties of individual  
21 amino acids on IDA-Cu(II) [33], strong binding amino acids histidine, tryptophan and  
22 phenylalanine were not found in excess amount in the identified motifs, however the strong  
23 binding amino acids glutamine, valine and leucine were routinely found. Tryptophan may  
24 therefore interfere with phage infection or phage protein amplification as Hansen et al. also  
25 described it to strongly bind to metal ions [34]. Differences in occurrence can of course be  
26 explained by different binding and elution conditions, which have a strong influence on  
27 retention and binding behavior [35]. Binding behavior of isolated phage was determined using  
28 the same conditions as used in biopanning. Binding efficiencies measured were found to be in  
29 a range of wild-type binding behavior to 18fold higher binding. Generally, motifs occurring  
30 with higher frequency showed an increased affinity towards nickel ions, however strongest  
31 binding motifs SMN06 and SMN12 were only found with a frequency of 01/29. These  
32 findings were discussed above and may be the result of several amplification steps favoring fast-  
33 propagating phage or slow-propagating phage [36–38]. Comparing motifs, originally  
34 identified to bind to nickel for their cobalt binding efficiencies and vice versa, we found that

1 sequences were identified, which preferred nickel over cobalt, although being identified as  
2 cobalt-binders. Additionally sequences were found, which bind to both metal ions equally  
3 good and those, which prefer cobalt. Also sequences were found, that bind to both metals  
4 worse compared to wild-type phage. Reasons for this are explained above. Generally we  
5 expected the identified sequences to bind to both metals as they show similar properties. Still,  
6 we could identify motifs, which selectively prefer one specific metal ion, even with  
7 experimental setup not discriminating between both, as no negative biopanning was carried  
8 out to prevent selection of fast-propagating off-target peptide sequences. Adaption of  
9 biopanning setup could easily lead to selection of motifs with even higher specificity.

10 *Conclusion.* In this study we demonstrated for both solid materials as e.g. CAT mineral and  
11 for heavy metal ions, that Phage Surface Display technology with appropriate biopanning  
12 conditions is suitable to identify peptide motifs, which bind to their target materials with high  
13 affinity and selectivity. Especially target material selection is nearly unlimited, promising  
14 wide application areas. We therefore propose the general usability of Phage Surface Display  
15 in resource technologies, opening completely new fields for biotechnological advances. These  
16 approaches are superior to conventional resource recovery technology especially comparing  
17 their ecological impact as in contrast no solid waste is produced and no harmful chemicals  
18 need to be used [39]. However, further characterization is needed to quantify process  
19 conditions, reusability and scale-up possibilities. Furthermore, for economic reasons,  
20 production of peptides most likely needs to be done by heterologous expression, which we  
21 could demonstrate to be simple and successful [40]. However, heterologously expressed  
22 peptides need to be carefully quantified with regard to their binding behavior and economic  
23 usability, as this may differ from phage binding results. In summary, we successfully  
24 transferred Phage Surface Display, until now mostly used for medical applications, to  
25 resource recovery, putting a new competitor on the market.

26

1 **Conflict of interest statement**

2 The authors declare that there is no conflict of interest.

3

1 **Acknowledgments.**

2 The authors of this study would like to thank Falk Lehmann and Katrin Flemming, their  
3 support has greatly appreciated. Special thanks to Dr. Jamie Scott for the pVIII phage library  
4 LX-4 and to Dr. Ulrich Soltmann from GMBU e.V. for providing materials and support for  
5 sol-gel synthesis.

6

## 1 **References.**

- 2 [1] Brierley CL. How will biomining be applied in future? *Trans Nonferrous Met Soc*  
3 *China* 2008;18:1302–10. doi:10.1016/S1003-6326(09)60002-9.
- 4 [2] Bosecker K. Bioleaching: metal solubilization by microorganisms. *FEMS Microbiol*  
5 *Rev* 1997;20:591–604. doi:10.1016/S0168-6445(97)00036-3.
- 6 [3] Johnson DB. Development and application of biotechnologies in the metal mining  
7 industry. *Environ Sci Pollut Res* 2013;20:7768–76. doi:10.1007/s11356-013-1482-7.
- 8 [4] Johnson DB. Biomining—biotechnologies for extracting and recovering metals from  
9 ores and waste materials. *Curr Opin Biotechnol* 2014;30:24–31.  
10 doi:10.1016/j.copbio.2014.04.008.
- 11 [5] Vera M, Schippers A, Sand W. Progress in bioleaching: fundamentals and mechanisms  
12 of bacterial metal sulfide oxidation—part A. *Appl Microbiol Biotechnol*  
13 2013;97:7529–41. doi:10.1007/s00253-013-4954-2.
- 14 [6] Sterritt RM, Lester JN. Interactions of heavy metals with bacteria. *Sci Total Environ*  
15 1980;14:5–17. doi:10.1016/0048-9697(80)90122-9.
- 16 [7] Schrader S, Kutschke S, Rudolph M, Pollmann K. Production of Amphiphilic  
17 Hydroxamate Siderophores Marinobactins by *Marinobacter* sp.  
18 DS40M6 for Bioflotation Process. *Solid State Phenom* 2017;262:413–6.  
19 doi:10.4028/www.scientific.net/SSP.262.413.
- 20 [8] Kuzmicheva GA, Belyavskaya VA. Peptide phage display in biotechnology and  
21 biomedicine. *Biochem (Moscow), Suppl Ser B Biomed Chem* 2017;11:1–15.  
22 doi:10.1134/S1990750817010061.
- 23 [9] Seker UOS, Demir HV. Material Binding Peptides for Nanotechnology. *Molecules*  
24 2011;16:1426–51. doi:10.3390/molecules16021426.
- 25 [10] Care A, Bergquist PL, Sunna A. Solid-binding peptides: smart tools for  
26 nanobiotechnology. *Trends Biotechnol* 2015;33:259–68.  
27 doi:10.1016/j.tibtech.2015.02.005.
- 28 [11] Bonnycastle LLC, Mehroke JS, Rashed M, Gong X, Scott JK. Probing the Basis of  
29 Antibody Reactivity with a Panel of Constrained Peptide Libraries Displayed by  
30 Filamentous Phage. *J Mol Biol* 1996;258:747–62. doi:10.1006/jmbi.1996.0284.

- 1 [12] Lederer FL, Curtis SB, Bachmann S, Dunbar WS, MacGillivray RTA. Identification of  
2 lanthanum-specific peptides for future recycling of rare earth elements from compact  
3 fluorescent lamps. *Biotechnol Bioeng* 2017;114:1016–24. doi:10.1002/bit.26240.
- 4 [13] Curtis SB, Hewitt J, MacGillivray RTA, Dunbar WS. Biomining with bacteriophage:  
5 Selectivity of displayed peptides for naturally occurring sphalerite and chalcopyrite.  
6 *Biotechnol Bioeng* 2009;102:644–50. doi:10.1002/bit.22073.
- 7 [14] Barbas CF. *Phage display : a laboratory manual*. Cold Spring Harbor Laboratory Press;  
8 2001.
- 9 [15] Schönberger N, Matys S, Flemming K, Lehmann F, Lederer FL, Pollmann K.  
10 Development of Metal Ion Binding Peptides Using Phage Surface Display Technology.  
11 *Solid State Phenom* 2017;262:591–5. doi:10.4028/www.scientific.net/SSP.262.591.
- 12 [16] Ploss M, Facey SJ, Bruhn C, Zemel L, Hofmann K, Stark RW, et al. Selection of  
13 peptides binding to metallic borides by screening M13 phage display libraries. *BMC*  
14 *Biotechnol* 2014;14:12. doi:10.1186/1472-6750-14-12.
- 15 [17] Matys S, Lederer FL, Schönberger N, Braun R, Lehmann F, Flemming K, et al. Phage  
16 Display - A Promising Tool for the Recovery of Valuable Metals from Primary and  
17 Secondary Resources. *Solid State Phenom* 2017;262:443–6.  
18 doi:10.4028/www.scientific.net/SSP.262.443.
- 19 [18] Gasteiger E, Hoogland C, Gattiker A, Duvaud S, Wilkins MR, Appel RD, et al. *Protein*  
20 *Identification and Analysis Tools on the ExPASy Server*. *Proteomics Protoc. Handb.*,  
21 Totowa, NJ: Humana Press; 2005, p. 571–607. doi:10.1385/1-59259-890-0:571.
- 22 [19] Hatanaka T, Matsugami A, Nonaka T, Takagi H, Hayashi F, Tani T, et al. Rationally  
23 designed mineralization for selective recovery of the rare earth elements. *Nat Commun*  
24 2017;8:15670. doi:10.1038/ncomms15670.
- 25 [20] Chen H, Su X, Neoh K-G, Choe W-S. QCM-D Analysis of Binding Mechanism of  
26 Phage Particles Displaying a Constrained Heptapeptide with Specific Affinity to SiO<sub>2</sub>  
27 and TiO<sub>2</sub>. *Anal Chem* 2006;78:4872–9. doi:10.1021/ac0603025.
- 28 [21] Chen C-L, Rosi NL. Peptide-Based Methods for the Preparation of Nanostructured  
29 Inorganic Materials. *Angew Chemie Int Ed* 2010;49:1924–42.  
30 doi:10.1002/anie.200903572.

- 1 [22] Derda R, Tang SKY, Li SC, Ng S, Matochko WL, Jafari MR. Diversity of Phage-  
2 Displayed Libraries of Peptides during Panning and Amplification. *Molecules*  
3 2011;16:1776–803. doi:10.3390/molecules16021776.
- 4 [23] Rodi DJ, Soares AS, Makowski L. Quantitative Assessment of Peptide Sequence  
5 Diversity in M13 Combinatorial Peptide Phage Display Libraries. *J Mol Biol*  
6 2002;322:1039–52. doi:10.1016/S0022-2836(02)00844-6.
- 7 [24] Menendez A, Scott JK. The nature of target-unrelated peptides recovered in the  
8 screening of phage-displayed random peptide libraries with antibodies. *Anal Biochem*  
9 2005;336:145–57. doi:10.1016/j.ab.2004.09.048.
- 10 [25] Vodnik M, Zager U, Strukelj B, Lunder M. Phage Display: Selecting Straws Instead of  
11 a Needle from a Haystack. *Molecules* 2011;16:790–817.  
12 doi:10.3390/molecules16010790.
- 13 [26] Baneyx F, Schwartz DT. Selection and analysis of solid-binding peptides. *Curr Opin*  
14 *Biotechnol* 2007;18:312–7. doi:10.1016/j.copbio.2007.04.008.
- 15 [27] Ueda EK., Gout P., Morganti L. Current and prospective applications of metal ion–  
16 protein binding. *J Chromatogr A* 2003;988:1–23. doi:10.1016/S0021-9673(02)02057-5.
- 17 [28] DeSilva TM, Veglia G, Porcelli F, Prantner AM, Opella SJ. Selectivity in heavy metal-  
18 binding to peptides and proteins. *Biopolymers* 2002;64:189–97.  
19 doi:10.1002/bip.10149.
- 20 [29] McConnell SI, Uveges AJ, Fowlkes DM, Spinella DG. Construction and screening of  
21 M13 phage libraries displaying long random peptides. *Mol Divers* 1996;1:165–76.  
22 doi:10.1007/BF01544954.
- 23 [30] Kotrba P, Dolecková L, de Lorenzo V, Ruml T. Enhanced bioaccumulation of heavy  
24 metal ions by bacterial cells due to surface display of short metal binding peptides.  
25 *Appl Environ Microbiol* 1999;65:1092–8.
- 26 [31] Porath J, Olin B. Immobilized metal ion affinity adsorption and immobilized metal ion  
27 affinity chromatography of biomaterials. Serum protein affinities for gel-immobilized  
28 iron and nickel ions. *Biochemistry* 1983;22:1621–30.
- 29 [32] Vançan S, Miranda EA, Bueno SMA. IMAC of human IgG: studies with IDA-  
30 immobilized copper, nickel, zinc, and cobalt ions and different buffer systems. *Process*

- 1 Biochem 2002;37:573–9. doi:10.1016/S0032-9592(01)00242-4.
- 2 [33] Yip T-T, Nakagawa Y, Porath J. Evaluation of the interaction of peptides with Cu(II),  
3 Ni(II), and Zn(II) by high-performance immobilized metal ion affinity  
4 chromatography. *Anal Biochem* 1989;183:159–71. doi:10.1016/0003-2697(89)90184-  
5 X.
- 6 [34] Hansen P, Lindeberg G. Purification of tryptophan containing synthetic peptides by  
7 selective binding of the  $\alpha$ -amino group to immobilised metal ions. *J Chromatogr A*  
8 1994;662:235–41. doi:10.1016/0021-9673(94)80510-5.
- 9 [35] Shiba K. Natural and artificial peptide motifs: their origins and the application of  
10 motif-programming. *Chem Soc Rev* 2010;39. doi:10.1039/b719081f.
- 11 [36] Rentero Rebollo I, Sabisz M, Baeriswyl V, Heinis C. Identification of target-binding  
12 peptide motifs by high-throughput sequencing of phage-selected peptides. *Nucleic*  
13 *Acids Res* 2014;42:e169. doi:10.1093/nar/gku940.
- 14 [37] Zanconato S, Minervini G, Poli I, De Lucrezia D. Selection dynamic of *Escherichia*  
15 *coli* host in M13 combinatorial peptide phage display libraries. *Biosci Biotechnol*  
16 *Biochem* 2011;75:812–5. doi:10.1271/bbb.110099.
- 17 [38] He B, Tjhung KF, Bennett NJ, Chou Y, Rau A, Huang J, et al. Compositional Bias in  
18 Naïve and Chemically-modified Phage-Displayed Libraries uncovered by Paired-end  
19 Deep Sequencing. *Sci Rep* 2018;8:1214. doi:10.1038/s41598-018-19439-2.
- 20 [39] Binnemans K, Jones PT, Blanpain B, Gerven T Van, Yang Y, Walton A, et al.  
21 Recycling of rare earths: a critical review. *J Clean Prod* 2013;51:1–22.  
22 doi:10.1016/j.jclepro.2012.12.037.
- 23 [40] Braun R, Matys S, Schönberger N, Lederer FL, Pollmann K. Simplified Expression  
24 and Production of Small Metal Binding Peptides. *Solid State Phenom* 2017;262:447–  
25 51. doi:10.4028/www.scientific.net/SSP.262.447.

26

27

1 **Tables**

2 Table 1: Summary of the occurrences of the selected, identified peptide sequences and their  
 3 general amino acid composition. R arginine, H histidine, K lysine, D aspartic acid, E glutamic  
 4 acid, S serine, T threonine, N asparagine, Q glutamine, C cysteine, G glycine, P proline, A  
 5 alanine, I isoleucine, L leucine, M methionine, F phenylalanine, W tryptophan, Y tyrosine, V  
 6 valine.

sequence motif		normalized binding efficiency	relative occurrence / frequency	competitive occurrence	theoretical pI	hydrophilic	hydrophobic	acidic	basic
KKQKCRTDACVTQM	SB1	128.6 ± 23.5	07/80	01/30	9.39	11	3	1	4
NEKKCKGARCTTVT	SB2	84.3 ± 19.4	03/80	03/30	9.39	11	2	1	4
ATPKCKKKSCMTTQ	SB3	94.5 ± 29.9	03/80	08/30	9.70	11	2	0	4
VDKKKSDDCGAWH			03/80	00/30	6.70	10	3	3	4
HDKKCKRQPCVLAN			02/80	01/30	9.39	10	3	1	5
FDKKCKSNKCLEVR			02/80	01/30	9.31	11	3	2	6
PKKKCHPEPCQTCG			02/80	01/30	8.77	10	0	1	4
KTEHCKKRKCPLDM			02/80	01/30	9.31	11	2	2	6
ETKKCTTGPCKVVT	SB4	13.4 ± 4.7	02/80	14/30	8.87	10	2	1	3
KKKKCKKKICTTHT			01/80	00/30	10.16	13	1	0	8
KKKKCKKNTCKNHT			01/80	00/30	10.16	14	0	0	8

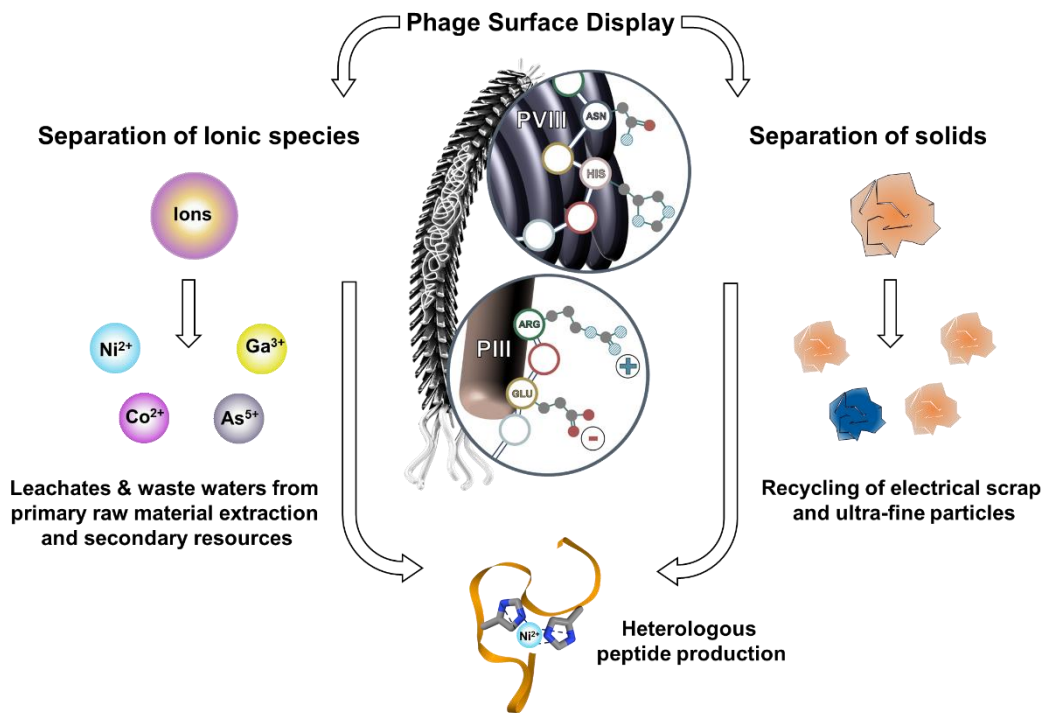
7

8

1 Table 2: Occurrence, general amino acid composition and theoretical pI (calculated with  
 2 ExPasy ProtParam) of selected, identified cobalt (A) and nickel (B) binding peptide sequences  
 3 using Phage Surface Display.

sequence motif		relative occurrence / frequency	normalized binding efficiency	theoretical pI	hydrophobic	charged	polar	aromatic	hydroxylic
<b>A Cobalt-binding peptide motifs</b>									
MSTGLSS	SMC01	28 / 63	2.8 ± 0.7	5.28	3	0	4	0	4
VPILEGT	SMC02	05 / 63	1.5 ± 0.3	4.00	5	1	1	0	1
DRTISNK	SMC03	02 / 63	1.8 ± 0.5	8.75	2	3	3	0	2
QNPNTL	SMC04	02 / 63	2.5 ± 0.9	5.52	3	0	4	0	1
SGTGASY	SMC05	02 / 63	1.7 ± 0.7	5.24	2	0	3	1	3
SSSVVTH	SMC06	02 / 63	2.3 ± 0.9	6.46	3	1	4	0	4
DAKDLNS	SMC07	01 / 63	2.5 ± 0.9	4.21	2	3	2	0	1
DNDTKAS	SMC08	01 / 63	1.5 ± 0.5	4.21	2	3	3	0	2
GLTDTSN	SMC09	01 / 63	0.8 ± 0.3	3.80	3	1	4	0	3
KTSTHAI	SMC10	01 / 63	1.5 ± 0.3	8.76	4	2	3	0	3
MRDSKML	SMC11	01 / 63	2.2 ± 0.6	8.50	3	3	1	0	1
STISKAK	SMC12	01 / 63	2.6 ± 0.8	10.00	3	2	3	0	3
TASQNFY	SMC13	01 / 63	1.4 ± 0.2	5.18	2	0	4	2	2
TGQGGEY	SMC14	01 / 63	1.5 ± 0.2	4.00	1	1	2	1	1
TKTQTHA	SMC15	01 / 63	0.8 ± 0.0	8.44	4	2	4	0	3
TNHSAYH	SMC16	01 / 63	2.7 ± 2.0	6.61	2	2	3	1	2
TQMLGQL	SMC17	01 / 63	1.4 ± 0.27	5.19	4	0	3	0	1
VSPNKEA	SMC18	01 / 63	3.1 ± 0.7	5.97	3	2	2	0	1
<b>B Nickel-binding peptide motifs</b>									
SGTGASY	SMN01	03 / 29	5.9 ± 1.7	5.24	2	0	3	1	3
MSTGLSS	SMN02	02 / 29	4.0 ± 2.9	5.28	3	0	4	0	4
NTGSPYE	SMN03	02 / 29	1.2 ± 0.0	4.00	2	1	3	1	2
TASQNFY	SMN04	02 / 29	10.4 ± 0.0	5.18	2	0	4	2	2
GSRSAQT	SMN05	01 / 29	2.0 ± 1.1	9.75	2	1	4	0	3
GTKGSLN	SMN06	01 / 29	17.8 ± 3.0	8.75	2	1	3	0	2
GYSSFNR	SMN07	01 / 29	3.6 ± 1.2	8.75	0	1	3	2	2
HHPVANT	SMN08	01 / 29	1.1 ± 0.2	6.92	4	2	2	0	1
HNETQKM	SMN09	01 / 29	1.6 ± 0.6	6.75	2	3	3	0	1
KDTSRSA	SMN10	01 / 29	1.2 ± 0.1	8.75	2	3	3	0	3
NAKHHPR	SMN11	01 / 29	16.8 ± 6.5	11.00	2	4	1	0	0
NGRAVNY	SMN12	01 / 29	0.9 ± 0.5	8.75	2	1	2	1	0
PGASVTY	SMN13	01 / 29	1.1 ± 1.0	5.95	4	0	2	1	2
RAEGTSE	SMN14	01 / 29	1.0 ± 0.0	4.53	2	3	2	0	2
RGATPMS	SMN15	01 / 29	1.0 ± 0.7	9.75	4	1	2	0	2
SLATDQK	SMN16	01 / 29	2.1 ± 0.8	5.55	3	2	3	0	2
SNNHSSM	SMN17	01 / 29	2.2 ± 1.0	6.46	1	1	5	0	3
STATPYK	SMN18	01 / 29	2.4 ± 1.5	8.31	4	1	3	1	3
TKTDVHF	SMN19	01 / 29	2.6 ± 2.0	6.41	3	3	2	1	2
TSVLNNT	SMN20	01 / 29	2.4 ± 0.4	5.19	4	0	5	0	3
VPILEGT	SMN21	01 / 29	1.9 ± 0.8	4.00	5	1	1	0	1

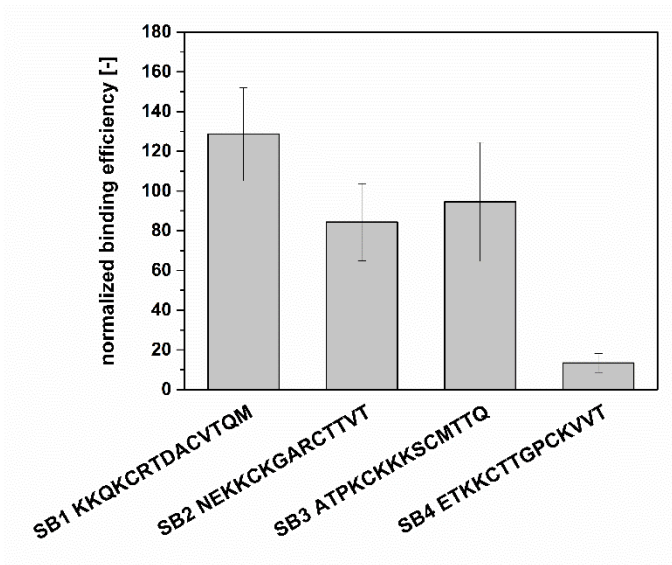
1 **Figures**



2

3 Fig. 1: Scheme of Phage Surface Display usage for biomining approaches. Peptides are used  
4 for separation of ionic species (left) and solids (right) and may be further optimized using  
5 genetic engineering for efficient heterologous production.

6

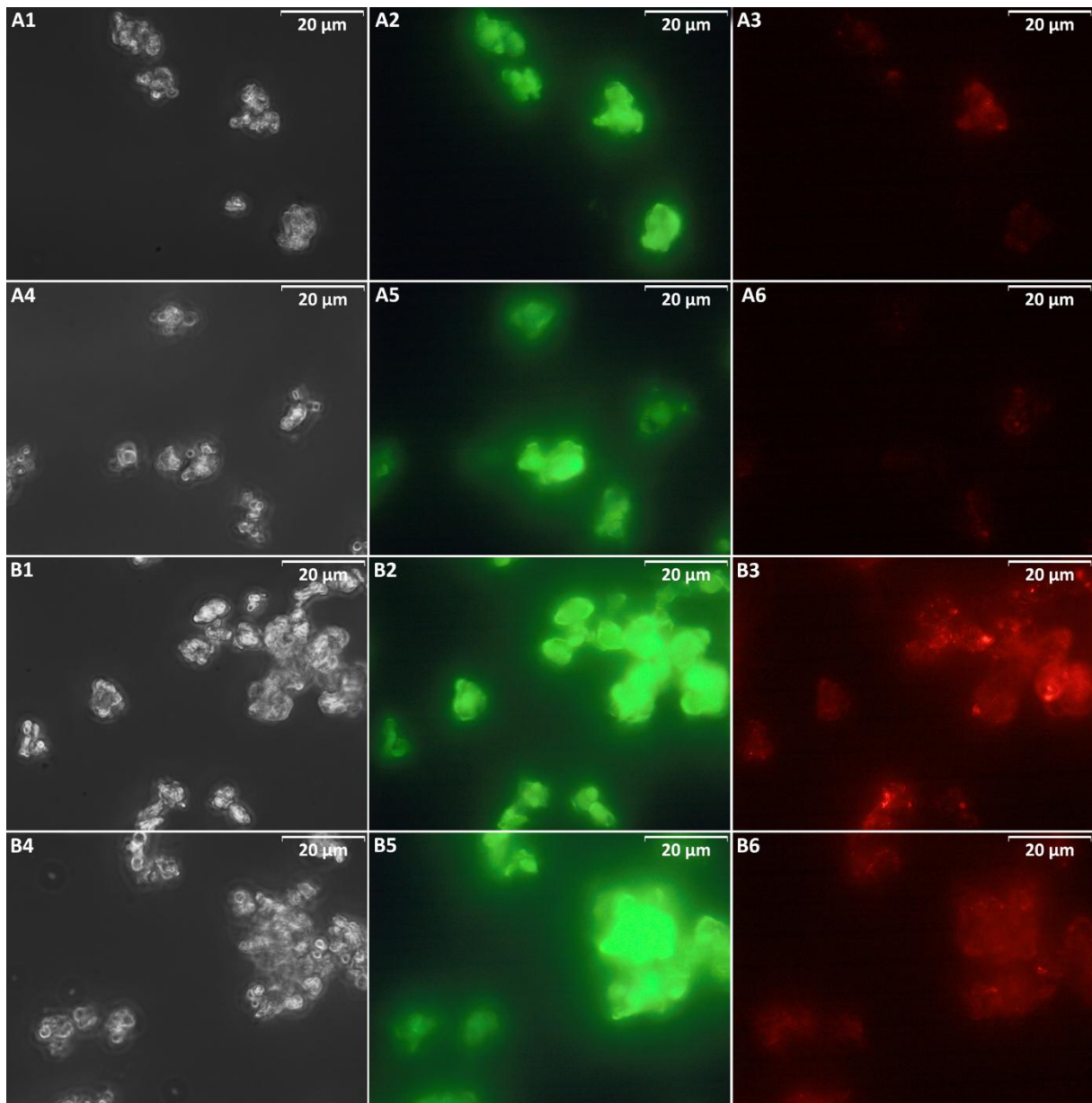


1

2 Fig. 2: Normalized results of the binding assays performed with CAT minerals and phage  
 3 displaying the shown amino acid sequences. Binding efficiency was calculated by  
 4 determining phage titer before and after binding and elution for selected phage. Results are  
 5 normalized against wild-type phage.

6

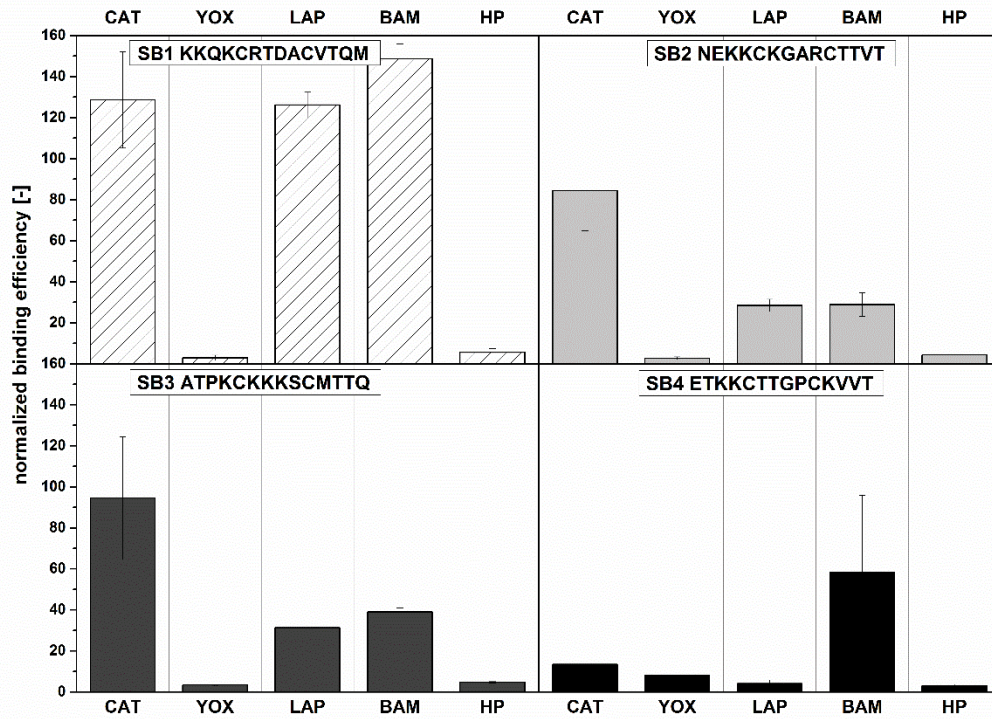
1



2

3 Fig. 3: Phase contrast (1,4) and fluorescence microscopy pictures (filter U-MNU 2, 5 and  
4 filter U-N39010 3,6) of phage displaying the sequence SB1 KKQKCRDQCVTQM (B) and  
5 wild-type phage (A) to CAT mineral. Pictures were taken after phage binding and antibody  
6 marking before elution of phage (1-3) and after elution of phage with elution buffer (4 – 6).

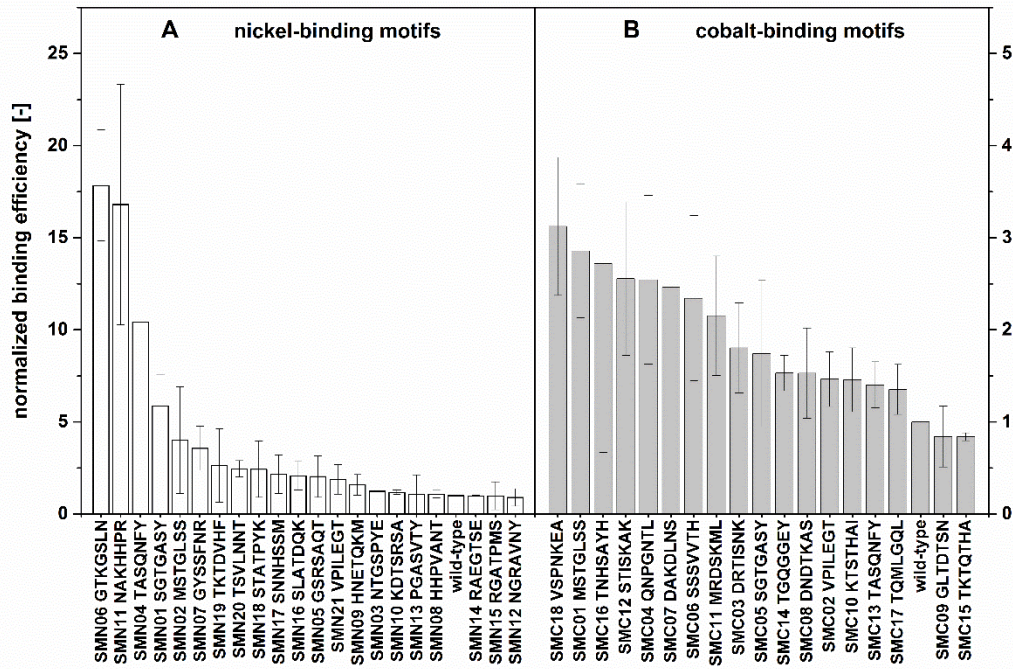
7



1

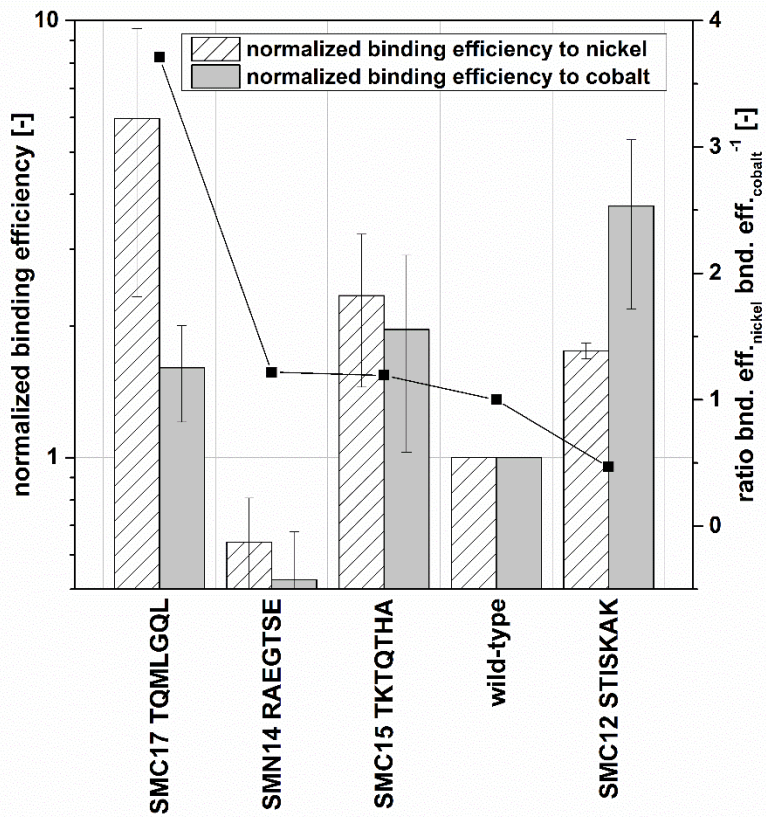
2 Fig. 4: Comparison of the binding efficiencies of four selected phage to different materials,  
 3 which are part of fluorescent lamp powder. Binding efficiency was calculated by determining  
 4 phage titer before and after binding and elution for selected phage normalized against wild-  
 5 type phage. Materials tested were CeMgAl11O19:Tb<sup>3+</sup> (CAT), Y2O3:Eu<sup>3+</sup> (YOX),  
 6 BaMgAl10O17:Eu<sup>2+</sup> (BAM), LaPO4:Ce,Tb (LAP) and halophosphate (HP).

7



1  
 2 Fig. 5: Normalized binding efficiencies of identified peptide motifs determined in comparison  
 3 of phage titer before and after binding and elution for selected phage normalized against wild-  
 4 type phage for nickel-binding sequences (A) and cobalt-binding sequences (B).

5



1

2 Fig. 6: Cross-binding of selected peptide motifs. Sequences found in nickel biopanning were  
 3 characterized for their binding efficiency towards cobalt and vice versa. Binding efficiencies  
 4 were determined as ratio of phage titer in input and eluate fractions of binding assays and  
 5 were normalized against the wild-type phage binding behavior. For comparison of nickel- and  
 6 cobalt-binding, the ratio of both binding efficiencies is shown.

Fig1

[Click here to download high resolution image](#)

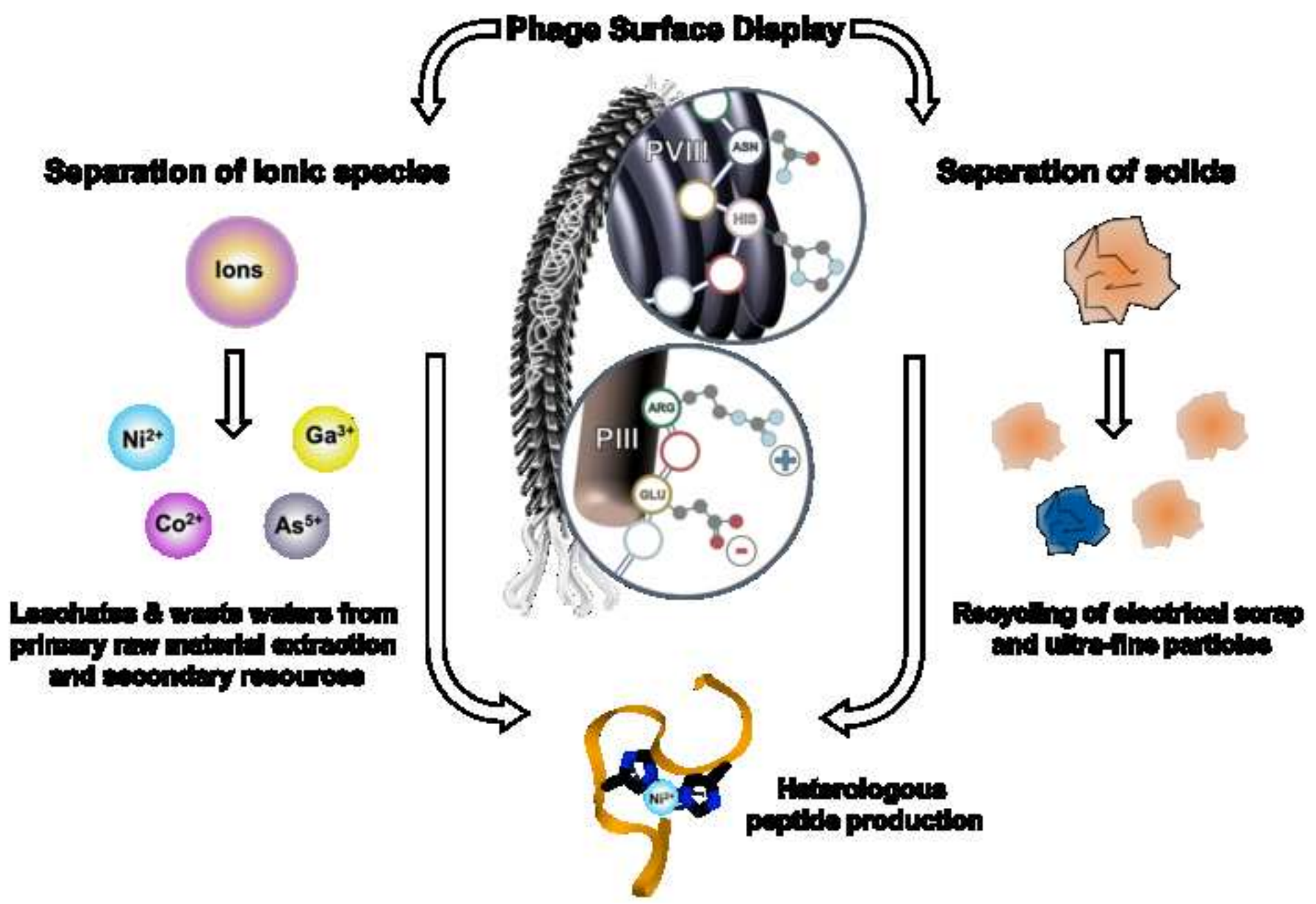


Fig2

[Click here to download high resolution image](#)

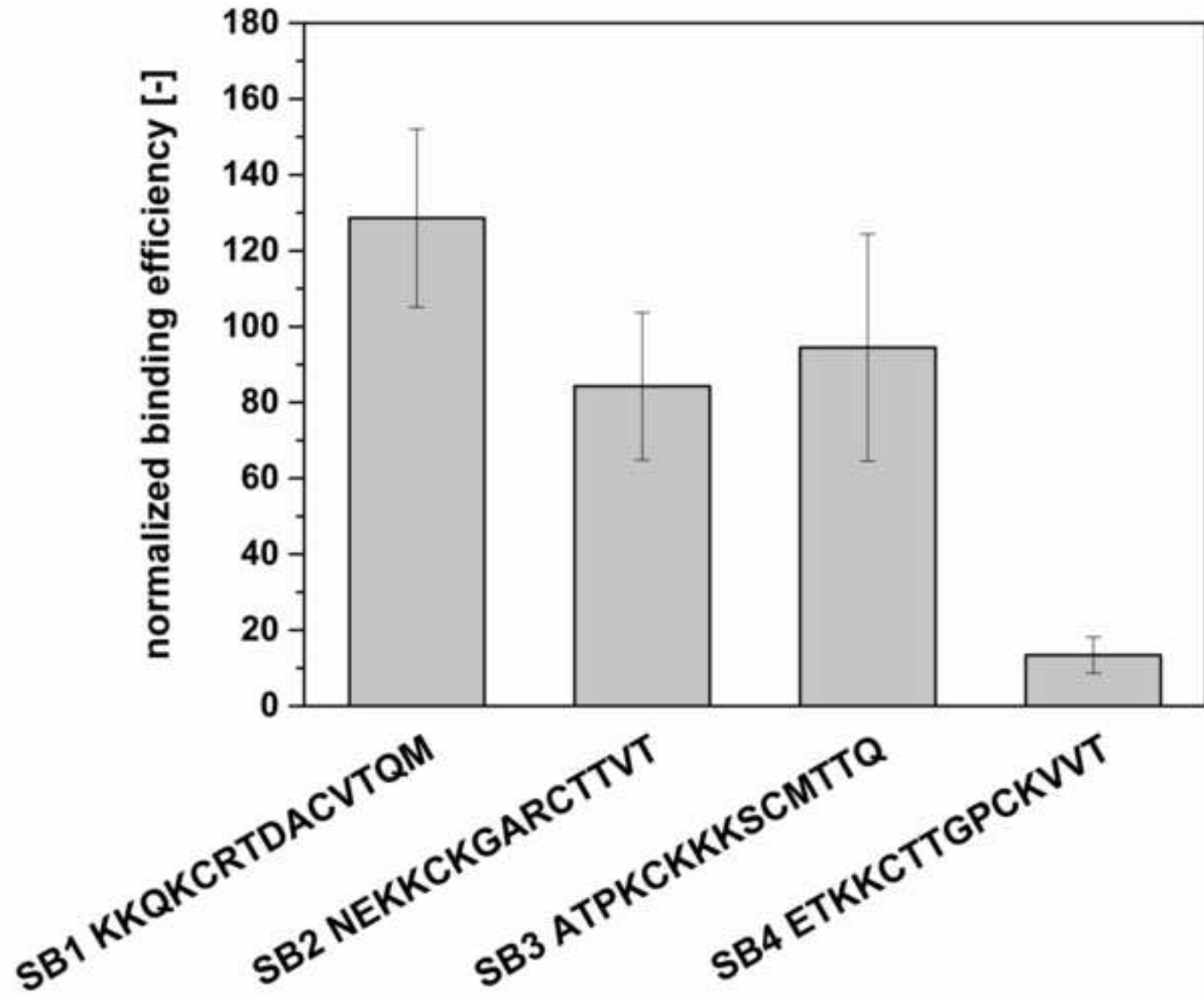


Fig3

[Click here to download high resolution image](#)

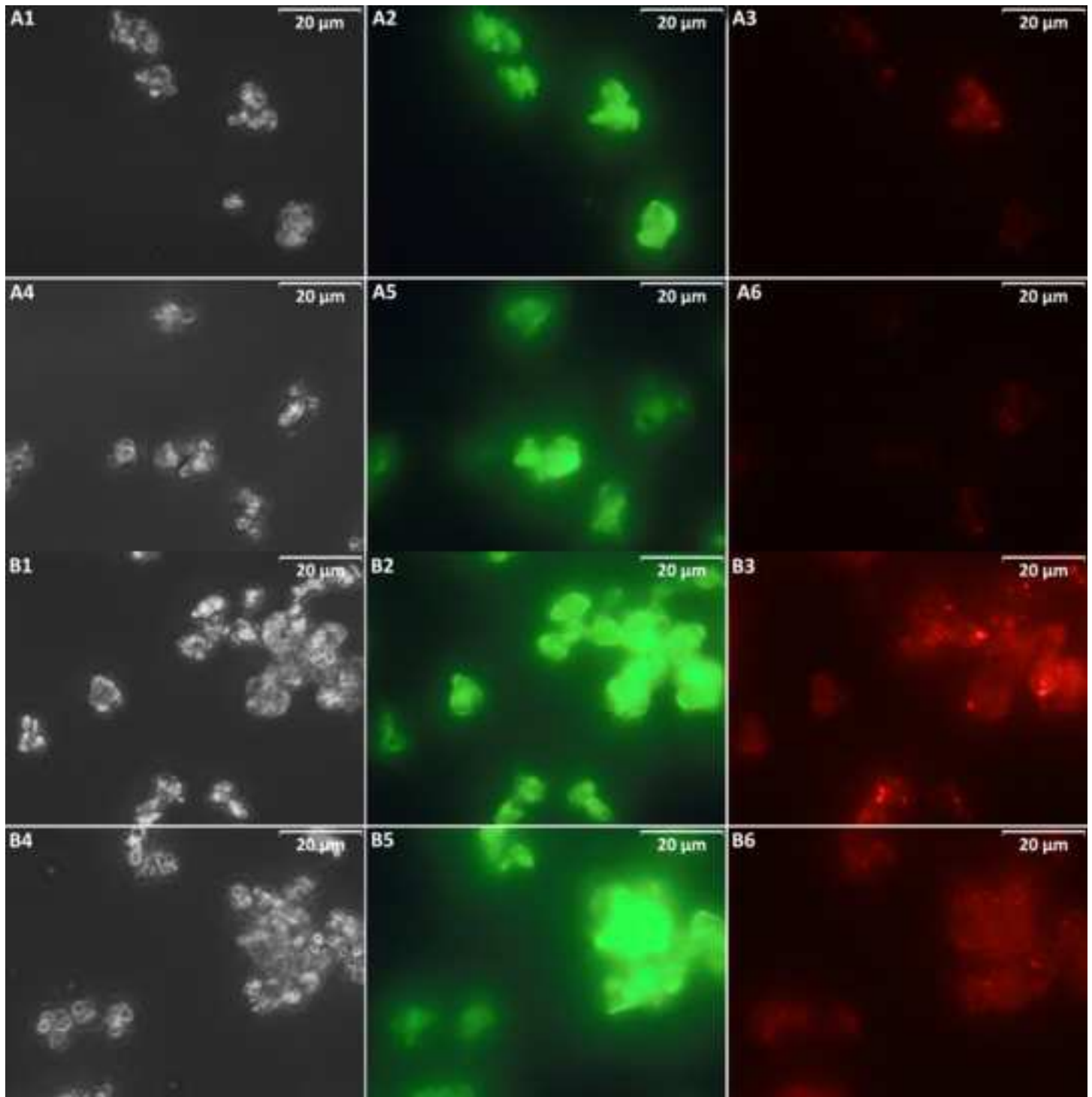


Fig4

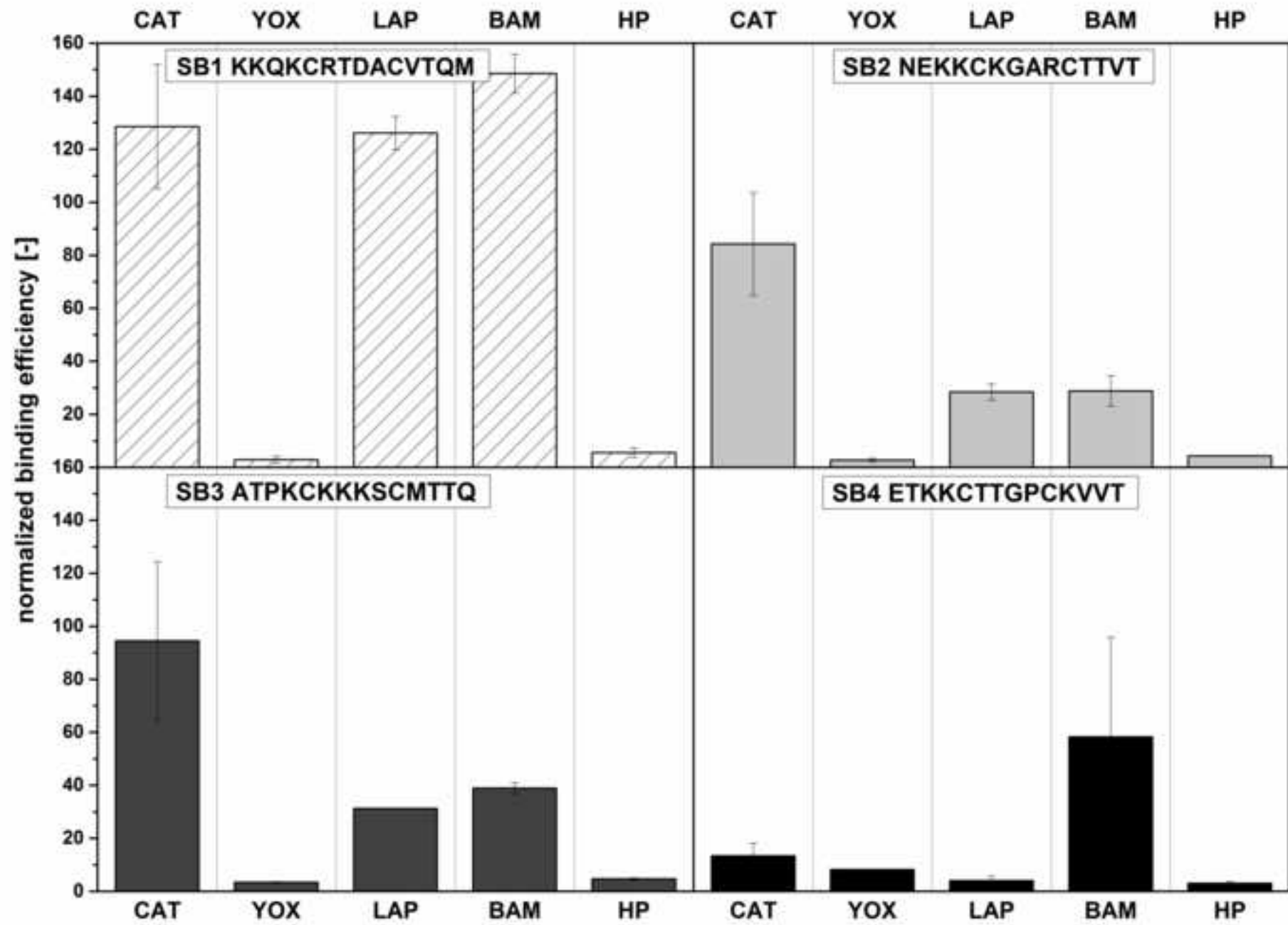
[Click here to download high resolution image](#)

Fig5

[Click here to download high resolution image](#)

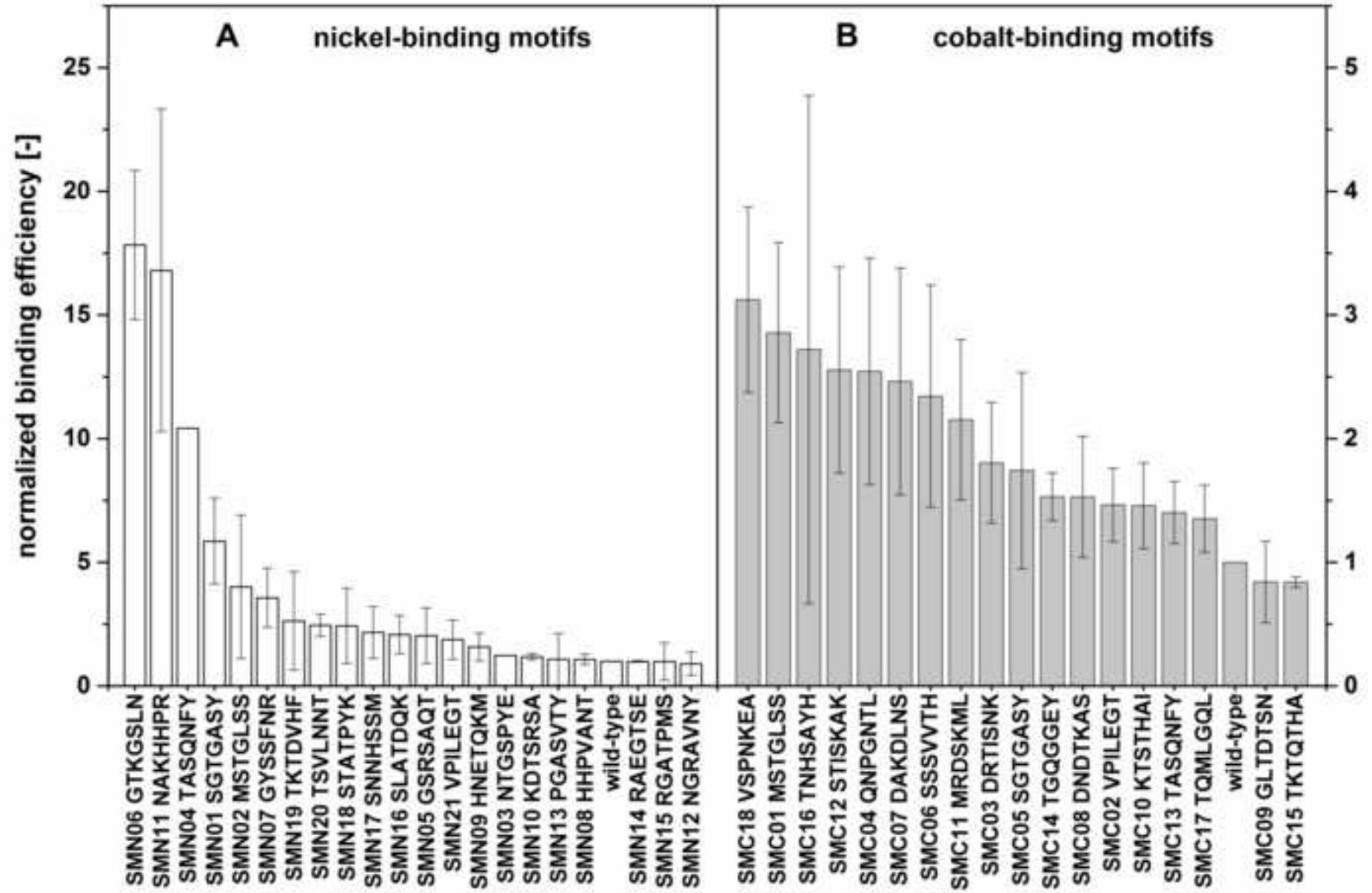


Fig6

[Click here to download high resolution image](#)